The property-governed activity of silver-modified titania photocatalysts: The influence of titania matrix

Kenta Yoshiiri [1,2], Baris Karabiyik [2], Kunlei Wang [2,3], Zhishun Wei [4], Christophe Colbeau-Justin [5] and Ewa Kowalska [1,2,*]

[1] Graduate School of Environmental Science, Hokkaido University, Sapporo, Japan

[2] Institute for Catalysis (ICAT), Hokkaido University, Sapporo, Japan

[3] Northwest Research Institute, Co. Ltd. of C.R.E.C., Lanzhou, China

[4] Hubei Provincial Key Laboratory of Green Materials for Light Industry, Hubei University of Technology, Wuhan, P.R. China; wei.zhishun@hbut.edu.cn (Z.W.)

[5] Laboratory of Physical Chemistry (LPC), Paris-Sud University, Orsay, France

***** Author to whom correspondence should be addressed: kowalska@cat.hokudai.ac.jp

ABSTRACT

Commercial titania photocatalysts were modified with silver nanoparticles (NPs) by photodeposition method in the presence/absence of methanol. The obtained photocatalysts were characterized by XRD, XPS, DRS, STEM and time-resolved microwave conductivity (TRMC) methods. The photocatalytic activity was tested under UV/vis irradiation for: (i) methanol dehydrogenation (during silver deposition), (ii) oxygen evolution with in-situ silver deposition, and (iii) oxidative decomposition of acetic acid, as well as under vis irradiation for 2-propanol oxidation. The action spectra of 2-propanol oxidation were also performed. It has been confirmed that modification of titania with silver causes significant improvement of photocatalytic activity under both UV and vis irradiation as silver works as an electron scavenger (TRMC data) and vis activator (possibly by an energy transfer mechanism). The obtained activities differ between titania samples significantly, suggesting that the type of crystalline phase, particle/crystallite sizes, and electron traps' density are crucial for both the properties of formed silver deposits and resultant photocatalytic activity. It might be concluded that under UV irradiation: (i) high crystallinity and large specific surface area are recommended for rutile- and anatase-rich samples, respectively, during hydrogen evolution, (ii) mixed crystalline phases cause high rate of oxygen evolution from water, and (iii) anatase phase with fine silver NPs results in efficient decomposition of acetic acid,

whereas under vis irradiation aggregated silver NPs (broad LSPR peak) on the rutile phase are promising for oxidation reactions.

I. INTRODUCTION

Photocatalysis under solar radiation has been considered as the possible solution for the most urgent human problems, i.e., energy, environment, and water. It is believed that application of highly efficient and stable photocatalysts with ability of working under broad range of solar radiation might be the best choice since it might operate without: (i) consumption of reagents, (ii) energy input, and (iii) formation of wastes, and thus could be considered as green and sustainable process. Among various photocatalysts, titanium(IV) oxide (titania) is probably the most widely investigated because of high activity, stability, abundance, low cost and negligible toxicity.[1-3] However, titania suffers from charge carriers' recombination (as all semiconductors) and inactivity under vis irradiation. Accordingly, various methods and procedures of its modification have been proposed, including surface modification,[4-6] doping,[7-9] coupling[10-12] and morphology architecture.[13-15] For example, modification with noble metals (NMs) results in double action, i.e., an activity enhancement under UV (NM working as an electron scavenger)[16-18] and vis response due to plasmonic properties.[19-23] Accordingly, NM-modified semiconductors with activity under vis irradiation, known as plasmonic photocatalysts, have been of great interest recently. It has been proposed that the proper design of their morphology, i.e., the size/shape (influencing the wavelengths of plasmonic peak) and the distribution of noble metal on the semiconducting support could result in high activity at broad range of irradiation.[22, 24-26] However, most studies have been performed for only one type of titania (or other semiconductors), and thus it is unknown how the properties of the support might influence the resultant properties of plasmonic photocatalysts and the overall activity. Our previous studies have shown the significant influence of titania matrix for gold-[24, 27] and copper-[28] modified samples, but only preliminary research has been done for silver ones.[29] Accordingly, here, eight different titania samples modified with the same content of silver (2 wt%) have been compared. Moreover, the conditions of silver photodeposition have been changed to investigate the influence of the properties of deposits on the resultant properties, and thus photocatalytic activity.

Additionally, the mechanism of plasmonic photocatalysis has not been clarified yet, and the energy transfer vs electron transfer have been mostly suggested.[19, 30-34] The morphology-dependent mechanism has also been proposed.[23, 35] It should be pointed out that in the case of silver and copper, the co-participation of other mechanisms is highly probable since these metals are easily oxidized, and thus formed oxides could form efficient heterojunction with titania (and other common photocatalysts).[28, 36-39] The stability of vis responsive photocatalysts must also be further investigated as proposed electron transfer (both in the case of plasmonic photocatalysis and coupled semiconductors) might result in oxidation and further release of

noble metal cations. Accordingly, this study is also focused on the stability issue during long-term irradiation, and the clarification of the possible mechanism for silver-modified titania photocatalysts.

II. METHODS

Eight titania samples, listed in Table 1, were modified with silver (2 wt% in respect to TiO_2) by photodeposition method. In brief, 0.6 g of titania was suspended in 25 mL of 50 vol% methanol-water solution in a Pyrex glass tube. Then, 2.2 mL of 50 mM $AgNO_3$ (99.8% Wako, Japan) was added under continuous stirring. Samples were also prepared in pure water (25 mL, Milli-Q) instead of methanol. The suspension was de-aerated by 15-min argon bubbling, and the tube was sealed with a rubber septum. Six samples could be prepared simultaneously by putting the tubes in a sample holder, placed around high-pressure Hg lamp in a thermostated water bath (25 °C), as shown in Fig. 1a. The tubes were irradiated under continuous stirring (500 rpm) for one hour, and 0.2 mL gas was sampled every 15 min to check the amount of evolved hydrogen or oxygen (methanol or water environment, respectively) by gas chromatography (GC-TCD). Then, other samples were also prepared for longer irradiation duration (5 h) in the presence of methanol. After irradiation, samples were washed at least three times with methanol and then three times with water, centrifuged, dried at 120 °C and ground in an agate mortar. The samples were named according to the titania type and the photodeposition conditions, where “w” and “m” mean that photodeposition was performed in water and methanol, respectively, whereas “1h” and “5h” correspond to the duration of irradiation. For example, AgP25m-1h states for silver-modified P25 titania by 1-h photodeposition of silver in methanol solution.

Samples were characterized by various methods, including X-ray diffraction (XRD, Rigaku Intelligent), X-ray photoelectron spectroscopy (XPS, JEOL, JP-9010MC), scanning transmission electron microscopy (STEM, Hitachi, HD 2000), energy-dispersive X-ray spectroscopy (EDS), and diffuse reflectance spectroscopy (DRS, Jasco, V-670). Time resolved microwave conductivity (TRMC) analysis was performed by an ns-time scale laser pulse (Nd:YAG with 10 Hz at 1064 nm and Gunn diode to generate 36.8 GHz microwave and laser pulses, respectively). Crystallinity of samples (Table 1) was estimated by internal standard method with nickel oxide (of 96% crystallinity) as a standard mixed thoroughly with titania (20:80 w/w) in an agate mortar before XRD analysis.[40]

Photocatalytic activity was examined under UV/vis irradiation (the same irradiation system as that used for photodeposition, except a sample holder, as shown in Fig. 1b) and vis irradiation (Xe lamp with cut-off filter) for oxidative decomposition of acetic acid and 2-propanol, respectively. In brief, 50 mg of sample was suspended in aqueous solution of acetic acid (5 vol%) or 2-propanol (5 vol%) and irradiated under continuous stirring. Generated products, i.e., carbon dioxide and acetone, were analyzed by gas

chromatography (GC-TCD and GC-FID, respectively). The action spectrum analysis was performed using diffraction-type illuminator for 2-propanol oxidation.

(a) (b)

FIG. 1. The photographs of UV/vis irradiation system for (**a**) samples' preparation, and (**b**) activity testing.

III. RESULTS

A. Synthesis of silver-modified titania samples

Silver was deposited on different titania samples (Table 1) via photodeposition method, i.e., under irradiation titania was excited (eq. 1), and thus photogenerated electrons reduced silver cations, forming zero-valent silver deposits directly on the titania surface. It has already been shown that photodeposition is one of the best methods for the fast and efficient (without metal loss) deposition of noble metals on various semiconductors.[18, 22, 24, 37] Here, to check how properties of silver deposits might influence the photocatalytic activity, two experimental conditions and different duration of irradiation ~~time~~ have been applied.

Table 1. The properties of titania samples used in this study

Titania name	Supplier	Composition (%)			Crystalline size*/nm	SSA/ $m^2\ g^{-1}$	ETs/ $\mu mol\ g^{-1}$
		anatase	rutile	NC phase			
ST01	Ishihara Sangyo Kaisha	73.7	0.0	26.3	8	298	84
FP6	CSJ	72.2	9.6	18.2	15	104	154
ST41	Ishihara Sangyo Kaisha	93.3	1.2	5.5	102	11	25
P25	Evonik Industries	76.6	13.3	10.1	22	59	50
UFR	Newcastle University	8.7	62.2	29.1	11	114	344
TIO6	CSJ	3.8	75.9	20.3	16	100	242
TIO5	CSJ	8.9	86.8	1.3	231	3	14
STG1	Showa Titanium	1.4	94.4	4.2	100	6	50

*the crystallite size of major component; CSJ – Catalysis Society of Japan; ETs – density of electron traps (data reported previously[40, 41]); NC – non-crystalline phase; SSA – specific surface area (data reported previously [40, 41])

First, silver was deposited in the presence of methanol as a hole scavenger (methanol dehydrogenation), as shown by the following equations (eq. 2-4). The progress of the reaction could be easily monitored by the estimation of the amount of evolved hydrogen on silver-modified titania (eq. 5).

$$TiO_2 \rightarrow TiO_2\,(e^-/h^+) \quad (1)$$

$$2Ag^+ + 2e^- \rightarrow 2Ag^0 \quad (2)$$

$$CH_3OH + 2h^+ \rightarrow HCHO + 2H^+ \quad (3)$$

$$2Ag^+ + CH_3OH \rightarrow 2Ag^0 + 2HCHO + 2H^+ \quad (4)$$

$$Ag/TiO_2 + CH_3OH \rightarrow Ag/TiO_2 + HCHO + H_2 \quad (5)$$

Next, pure water was used as a hole scavenger (water oxidation), according to the following equations (eq. 6-8), and the progress of reaction could be monitored by estimation of the amount of evolved oxygen.

$$2Ag^+ + 2e^- \rightarrow 2Ag^0 \quad (6)$$

$$H_2O + 2h^+ \rightarrow 1/2O_2 + 2H^+ \quad (7)$$

$$2Ag^+ + H_2O \rightarrow Ag^0 + 1/2O_2 + 2H^+ \quad (8)$$

The obtained results of hydrogen and oxygen generation during silver photodeposition on different titania samples are shown in Fig. 2. Interestingly, in the case of methanol dehydrogenation (Fig. 2a), the highest photocatalytic activity is observed for large rutile (STG1 and TIO5) and fine anatase (ST01) samples. Similar phenomenon has also been observed for gold-modified titania photocatalysts, where the highest activities among 15 titania samples were obtained when gold was deposited on ST01 and TIO5 titania photocatalysts.[22, 27] In the case of anatase samples, the activity dropped with an increase in the particle size (a decrease in specific surface area), whereas an opposite situation was observed for rutile samples.[27] Considering, another study for 35 different titania samples, tested in four different reactions systems, it has been found that both high crystallinity (low content of crystal defects – electron traps) and high specific surface area are preferable for methanol dehydrogenation with in-situ platinum deposition.[40] Accordingly, it might be concluded that also for in-situ silver photodeposition, high crystallinity and large specific surface area are key factors for hydrogen evolution on rutile- and anatase-based samples, respectively.

In contrast to the methanol dehydrogenation case, the water oxidation with in-situ silver deposition is characterized by much lower efficiency, as shown in Fig. 2b. This is not surprising as high overpotential

(resulting from the first step of proton removal)[42] and low efficiency are commonly reported as the main reasons of slow oxygen evolution. The contradictory data could be found in the literature, suggesting that (i) rutile is an active phase of titania (especially with large particle sizes),[43-46] (ii) inactivity of rutile,[47] and (iii) the synergism between anatase and rutile.[45, 47] Kakuma et al. have proposed that rutile could form a Ti–OO–Ti surface structure (as the distance between titanium atoms on the surface of rutile is smaller than that on anatase one), resulting in high efficiency of O_2 formation.[48] Interestingly, even though commercial rutile showed the highest activity, the different behavior was observed for self-prepared samples, where the sample with the highest anatase-to-rutile ratio exhibited the best performance (but only three different compositions were tested, i.e., 57.8%, 73.1% and 88.8% of anatase).[45] Similarly, here, P25 sample has been the most active (with ca. 85% anatase content), but both the presence of large rutile particles (40-130 nm)[49] and the synergism between both phases could be responsible for observed effect.

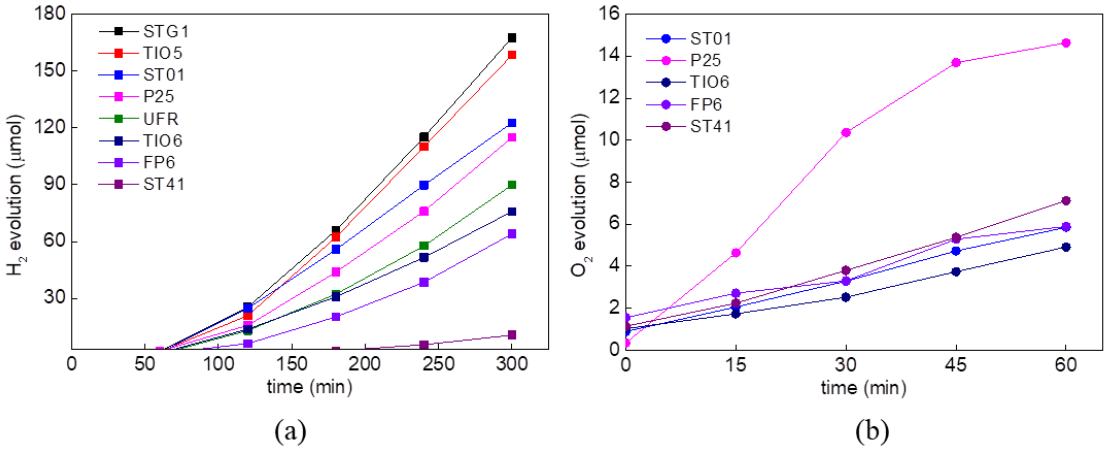

FIG. 2. Evolution of (**a**) hydrogen, and (**b**) oxygen during silver deposition on titania samples.

B. Characterization of silver-modified titania samples

During silver photodeposition, the color of fine titania (ST01, FP6, P25 and TIO6) has changed from white to brown/yellow (Table 2), which confirms that silver is reduced, forming zero-valent deposits on the titania surface. In the case of titania photocatalysts with large particles (ST41, STG1 and TIO5), the color turned to violet, which indicates the formation of larger silver particles. The localized surface plasmon resonance (LSPR) of silver appears at ca. 395-405 nm (brown color) for fine silver NPs (5-10 nm), and bathochromic shift is observed with an increase in the NPs' sizes, e.g., LSPR at 500 nm (violet color) for 100-nm NPs.[50, 51] Accordingly, it might be concluded that the properties of titania influence the properties of deposited silver, i.e., the larger the titania NP is, the larger are formed NPs of silver. Similar observation

has already been found for gold-modified titania, where a linear dependence between crystallite sizes of gold and titania has been observed.[22] It is thought that the preferential deposition of metallic NPs on the surface defects of titania[52] could be the main reason of this behavior as fine titania samples are characterized by high density of surface defects (electron traps, ETs).[53, 54]

However, in contrast to gold-modified titania samples, the color of silver ones is not stable, and its change after samples' drying is observed, as presented in Table 2 and Fig. 3. Similar data have already been reported for other silver-modified titania samples (and also other photocatalysts modified with less noble metals, such as copper),[28, 37, 38] and it has been thought that the color change results from the partial surface oxidation of silver deposits.[29, 55] Obviously, DRS spectra (exemplary data for anatase ST41 and rutile TIO5 shown in Fig. 3) confirm that vis response has been achieved in the case of all modified titania samples in respect to the pristine titania samples with absorption edges at ca. 390-420 nm (black lines) depending on the polymorphic form. The modified samples exhibit two peaks in DRS spectra at vis range (Figs. 3b and 3d) due to the silver presence. The peak at shorter wavelengths (ca. 390-420 nm; clearly shown in Figs. 3b and 3d) suggests the presence of zero-valent silver, whereas photoabsorption at longer wavelengths (520-570) might be caused by oxidized forms of silver. Similar photoabsorption properties have been observed for titania samples modified with silver(I) oxide.[56]

Table 2. The color of titania samples during/after silver photodeposition

Sample name	ST01	FP6	ST41	P25	UFR	TIO6	STG1	TIO5
during silver photodeposition								
Ag(TiO_2)m-1h	d. brown	yellow	l. violet	d. yellow	d. brown	d. brown/violet	violet	violet
Ag(TiO_2)w-1h	d. brown	l. brown	l. violet	l. brown	violet	violet	violet	violet
Ag(TiO_2)m-5h	d. brown	d. yellow	l. brown	d. yellow	d. brown	d. brown	violet	violet
after silver photodeposition (dried samples)								
Ag(TiO_2)m-1h	l. brown	brown	violet	l. brown	gray	gray	violet/gray	violet/gray
Ag(TiO_2)w-1h	l. yellow	l. brown	l. violet	v.l. brown	gray	l. gray	violet	violet/gray
Ag(TiO_2)m-5h	creamy	l. brown	violet	gray	gray	gray	violet	violet/gray

d – dark; l – light; v.l. – very light

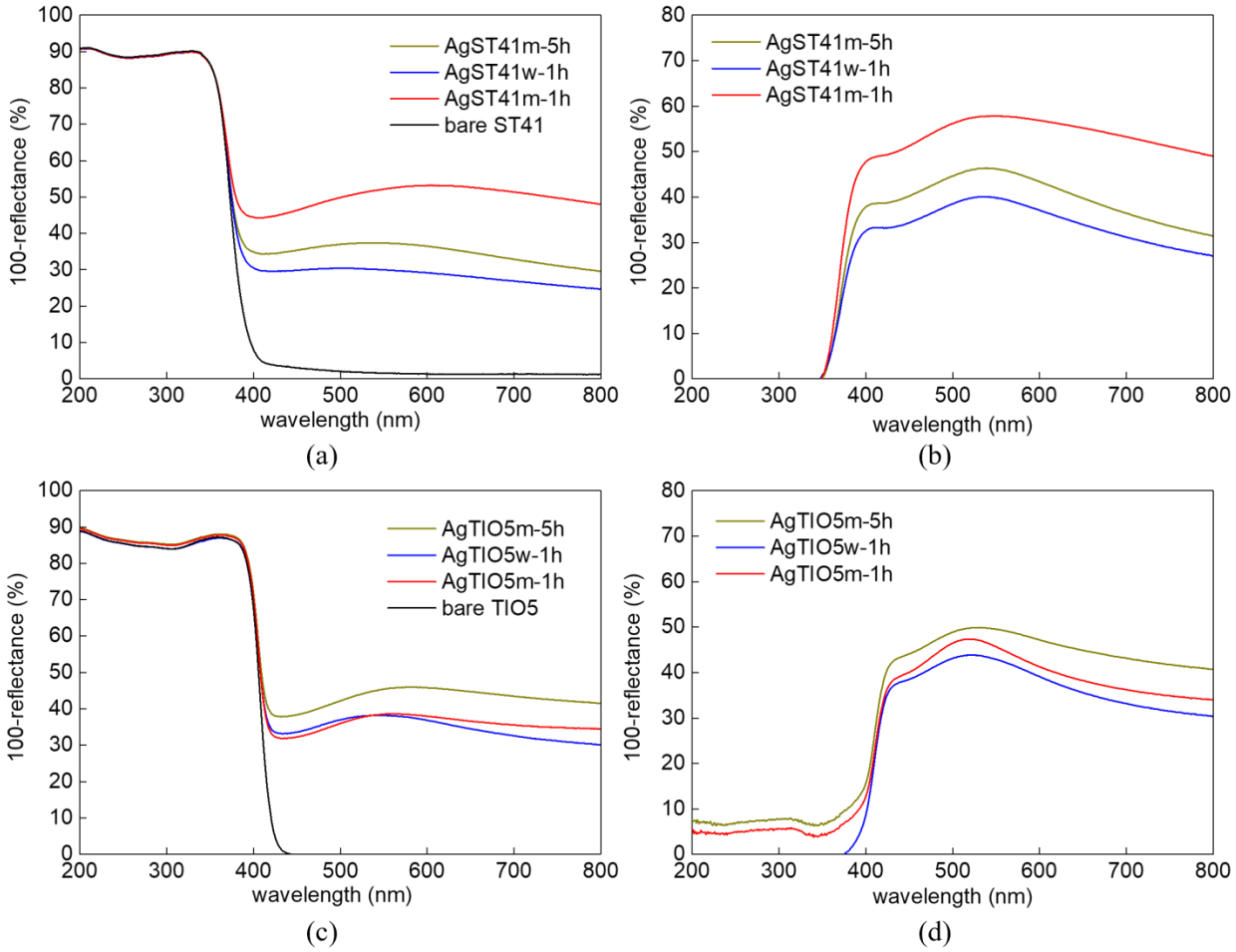

FIG. 3. Exemplary DRS data for pristine and silver-modified titania samples: anatase ST41 (**a**-**b**) and rutile TIO5 (**c**-**d**) taken with $BaSO_4$ (**a**, **c**) and respective pristine titania (**b**, **d**) as references.

The crystal properties of obtained samples have been analyzed by XRD, and exemplary data are shown in Fig. 4 and Table 3. Indeed, the presence of silver has been confirmed in all modified samples. Moreover, in general the larger deposits have been formed on the titania samples with larger particles, as already suggested from the color of samples. It should be pointed out that only crystallites could be analyzed by XRD, and thus non-crystalline deposits (e.g., with mixed oxidate states) could not be detected. Moreover, the low content of phases and the crystallites of small sizes are also difficult for detection. Therefore, all these issues should be considered when analyzing the properties of obtained samples.

The deposition of larger and more polydisperse NPs of silver on titania samples with larger particles has been further confirmed by STEM observations, as shown in Fig. 5. Generally, spherical NPs of silver has been formed, but some rod-like deposits in the case of large titania have also been observed. In the case of fine titania, very fine silver NPs (even nano-sized NPs in the case of AgST01m-5h) with the average

particle size of 5.3 ± 2.4 nm have been synthesized, whereas both very fine and large NPs (> 60 nm) in the case of larger titania.

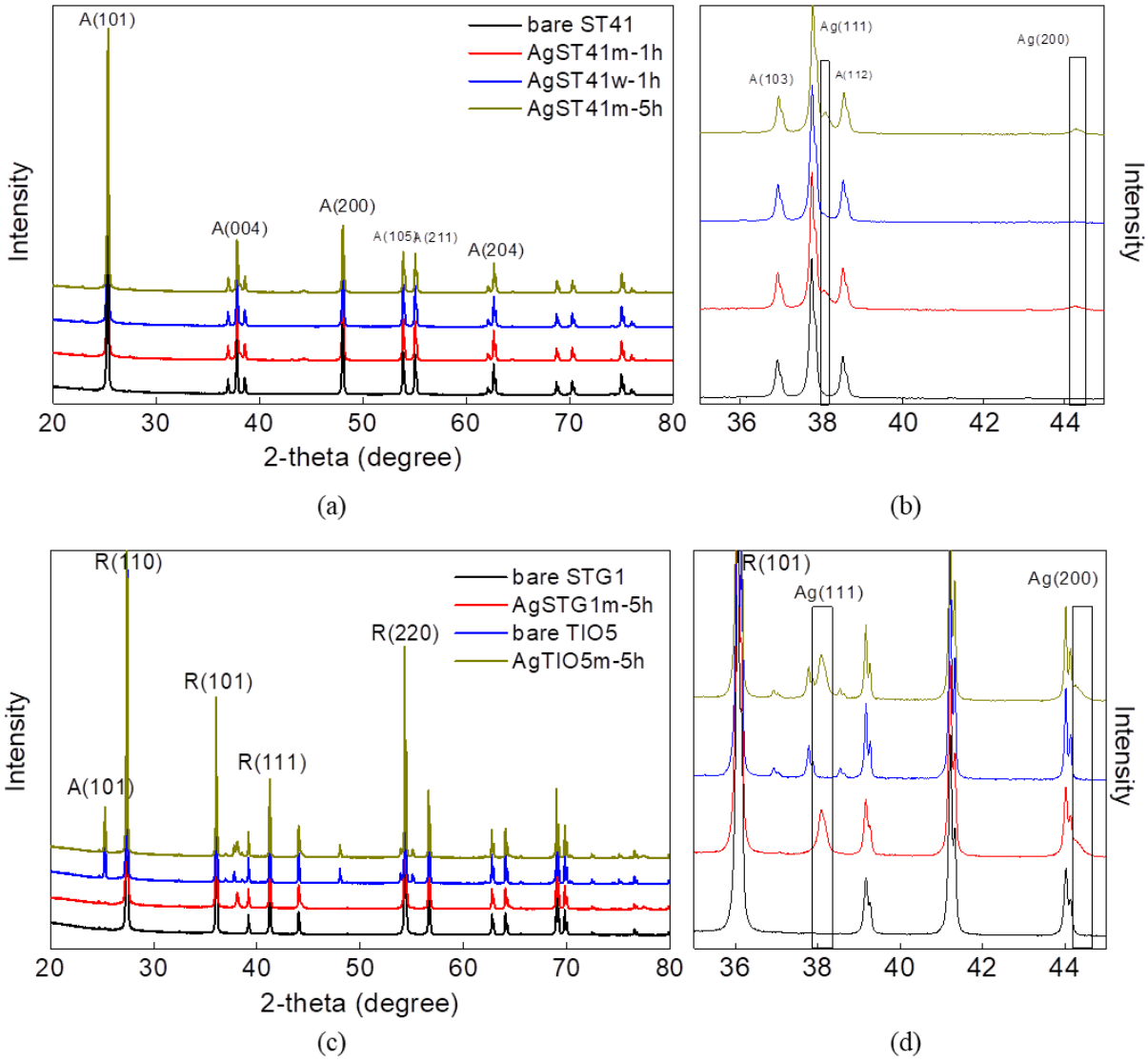

FIG. 4. Exemplary XRD data for pristine and silver-modified titania samples: (a-b) anatase ST41 and (c-d) large rutile samples (STG1 and TIO5) prepared during 5-h methanol dehydrogenation; magnified patterns for narrow range of angles (to show silver peaks) are presented on the right site (as b and d, respectively).

Table 3. The crystalline properties of silver-modified titania

Sample name	crystalline content (wt%)				crystalline size (nm)		
	TiO_2	Ag^0	Ag_2O	AgO	Ag^0	Ag_2O	AgO
AgST01m-1h	97.2	1.3	N.D.	1.5	4.1	-	2.0
AgST01w-1h	98.8	0.2	0.4	0.6	14.2	-	10.6
AgST01m-5h	99.4	0.5	N.D.	0.1	4.7	-	-
AgFP6m-1h	99.4	0.2	0.3	0.1	6.3	0.8	-
AgFP6w-1h	98.6	0.3	0.5	0.6	26.2	9.5	9.2
AgFP6m-5h	95.9	3.0	1.1	N.D.	1.3	1.3	-
AgST41m-1h	98.6	1.2	N.D.	0.2	30.7	-	-
AgST41w-1h	99.9	0.1	N.D.	N.D.	-	-	-
AgST41m-5h	98.7	1.1	N.D.	0.2	44.3	-	-
AgUFRm-1h	97.5	1.1	1.0	0.4	4.6	4.7	7.7
AgUFRw-1h	99.3	0.2	0.1	0.4	-	2.1	2.0
AgUFRm-5h	98.7	1.1	N.D.	0.2	-	8.7	-
AgTiO6m-1h	97.5	0.6	1.2	0.7	4.5	1.1	3.6
AgTIO6w-1h	96.2	1.6	2.2	N.D.	0.7	1.6	-
AgTIO6m-5h	99.3	0.6	0.1	N.D.	23.1	15.5	-
AgTIO5m-1h	98.9	0.7	0.1	0.3	5.5	-	9.8
AgTIO5w-1h	98.6	1.9	0.1	0.4	58.2	-	0.9
AgTIO5m-5h	95.8	1.7	0.4	2.1	27.5	-	-
AgSTG1m-1h	96.5	2.9	0.6	N.D.	12.9	3.4	-
AgSTG1w-1h	96.9	1.6	1.5	N.D	27.3	5.0	-
AgSTG1m-5h	97.5	1.7	0.3	0.5	57.4	-	-

N.D. – not detected

Next, the surface properties of silver deposits have been investigated by XPS analysis, and exemplary data for samples containing large anatase (ST41) are shown in Fig. 6. As expected, silver on the surface exists mainly in the oxidized form, i.e., monovalent (1+) being the majority state, reaching the lowest and the highest content of 66.3% and 88.7% in the case of AgP25m-1h and AgST41m-1h, respectively. The summarized data for all analyzed samples are presented in Table 4. Interestingly, even though silver has been partly oxidized (XPS can estimate only surface composition.), zero-valent silver is still present in all analyzed samples.

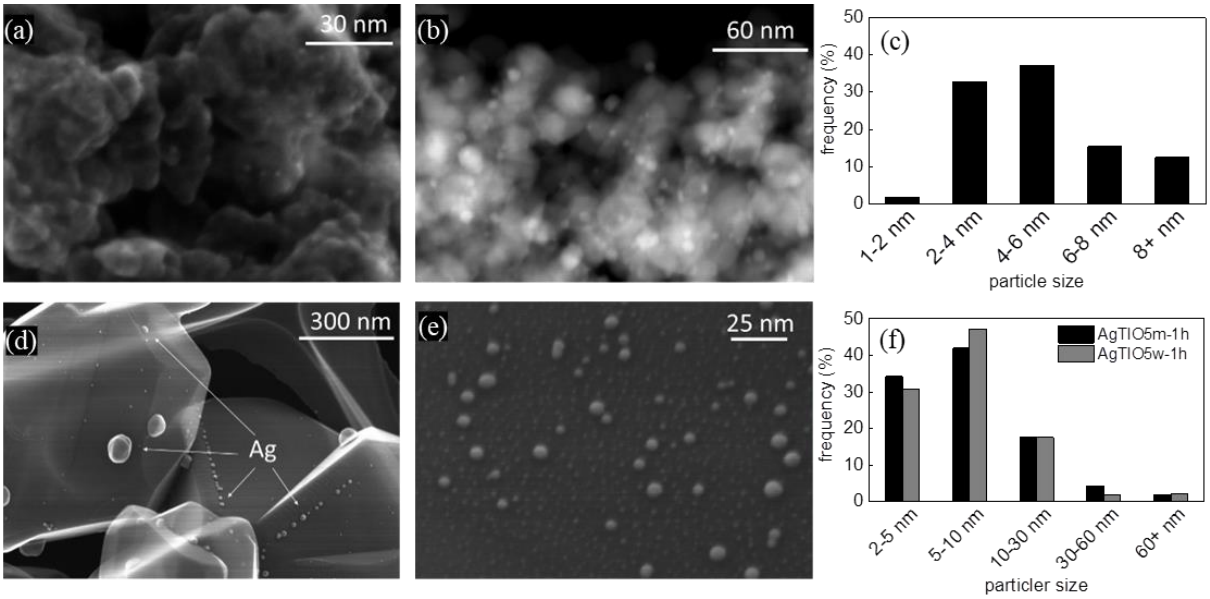

FIG. 5. Morphology observation of silver-modified titania: (**a**, **b**, **d**, **e**) STEM images of: (**a**) AgST01m-5h, (**b**) AgP25m-1h and (**d**-**e**) AgTIO5m-1h; (**c**, **f**) distribution of silver NPs in (**c**) AgP25m-1h and (**f**) AgTIO5m-1h.

Table 4. The content of different oxidation forms of silver (%) in silver-modified titania samples

Sample	Ag^0	Ag^+	Ag^{2+}
AgST01m-5h	22.2	74.1	3.7
AgFP6m-1h	8.3	80.7	11.0
AgST41m-1h	8.7	88.7	2.6
AgST41w-1h	9.4	85.8	4.8
AgST41m-5h	10.8	86.0	3.2
AgP25m-1h	30.6	66.3	3.1
AgP25m-5h	22.7	70.6	6.68
AgUFRm-1h	21.9	73.5	4.6
AgTIO6m-5h	7.1	82.9	10.0
AgTIO5m-1h	9.1	81.7	9.2
AgTIO5w-1h	17.5	79.1	3.4
AgSTG1m-5h	16.5	80.8	2.7

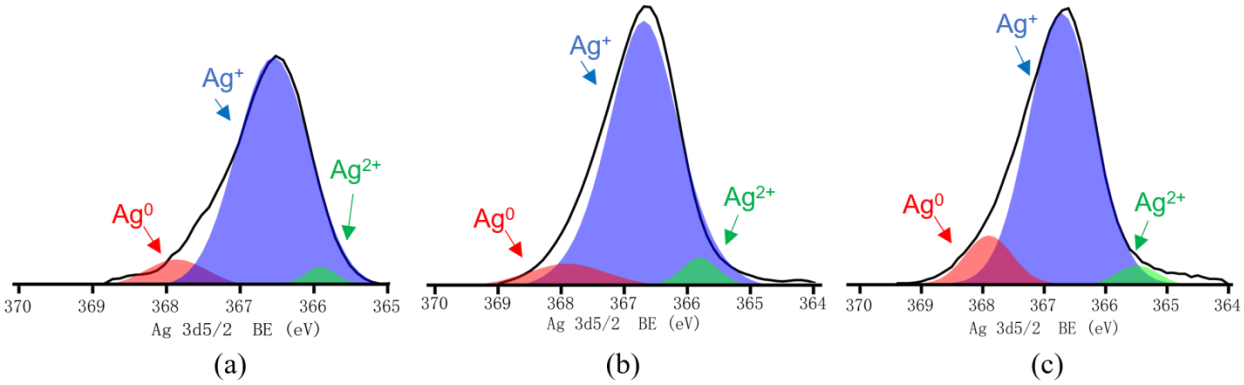

FIG. 6. XPS data of Ag $3d_{5/2}$ for (**a**) AgST41m-1h, (**b**) AgST41w-1h, and (**c**) AgST41m-5h.

C. Photocatalytic activity of silver-modified titania samples

First, photocatalytic activity of all samples was investigated under UV/vis irradiation for oxidative decomposition of acetic acid, and obtained results are shown in Fig. 7a. The modification of anatase-rich samples with silver results in 2-4 fold increase in photocatalytic activity, as shown in Fig. 7a. The most active samples are those based on large anatase, i.e., ST41 and P25. To investigate the possible reason of activity enhancement, the time-resolved microwave conductivity (TRMC)[57] method was used. Three samples (pristine and modified ST01) were excited at fixed wavelength of 355 nm. The significant decrease in the intensity of TRMC signal (Fig. 7c-d) for silver modified samples has confirmed that silver works as an electron scavenger, inhibiting charge carriers' recombination. The conditions of silver photodeposition have slight impact on the photocatalytic activity, and it is clear that extended duration of photodeposition has inhibited the activity. The decrease in activity could be caused by silver aggregation, similar to reported gold-modified titania case,[58] and thus a decrease in the number of active sites. On the other hand, much different bahaviour has been observed for rutile-rich samples, where silver deposition does not change (TIO6), reduces (UFR) or increaseas (TIO5) the photocatalytic activity. Much lower activity of rutile than anatase has been comonnly reported, especially in the case of oxidation reactions, with various possible reasons, i.e., (i) the direct bandgap leading to fast recombination of charge carriers, (ii) less positive valence band, (iii) larger content of deep ETs, etc.[40, 54, 59-61] Moreover, the particle size of titania might also influence the photocatalytic activity. Usually, titania with large particles are highly crystallized, and thus with low content of defects. Indeed, ST41, TIO5 and STG1 contain almost pure crystalline phases and very low density of ETs, as shown in Table 1. In addition, diffuse reflectance spectra of the reaction suspension (photocatalyst in aqueous acetic acid) have been taken before and during the irradiation for one of the most

active samples (AgST41w-1h). It is clear that UV/vis irradiation (even 2 min) has caused re-apperance of silver plasmonic peak with max at ca. 470 nm (Fig. 7b).

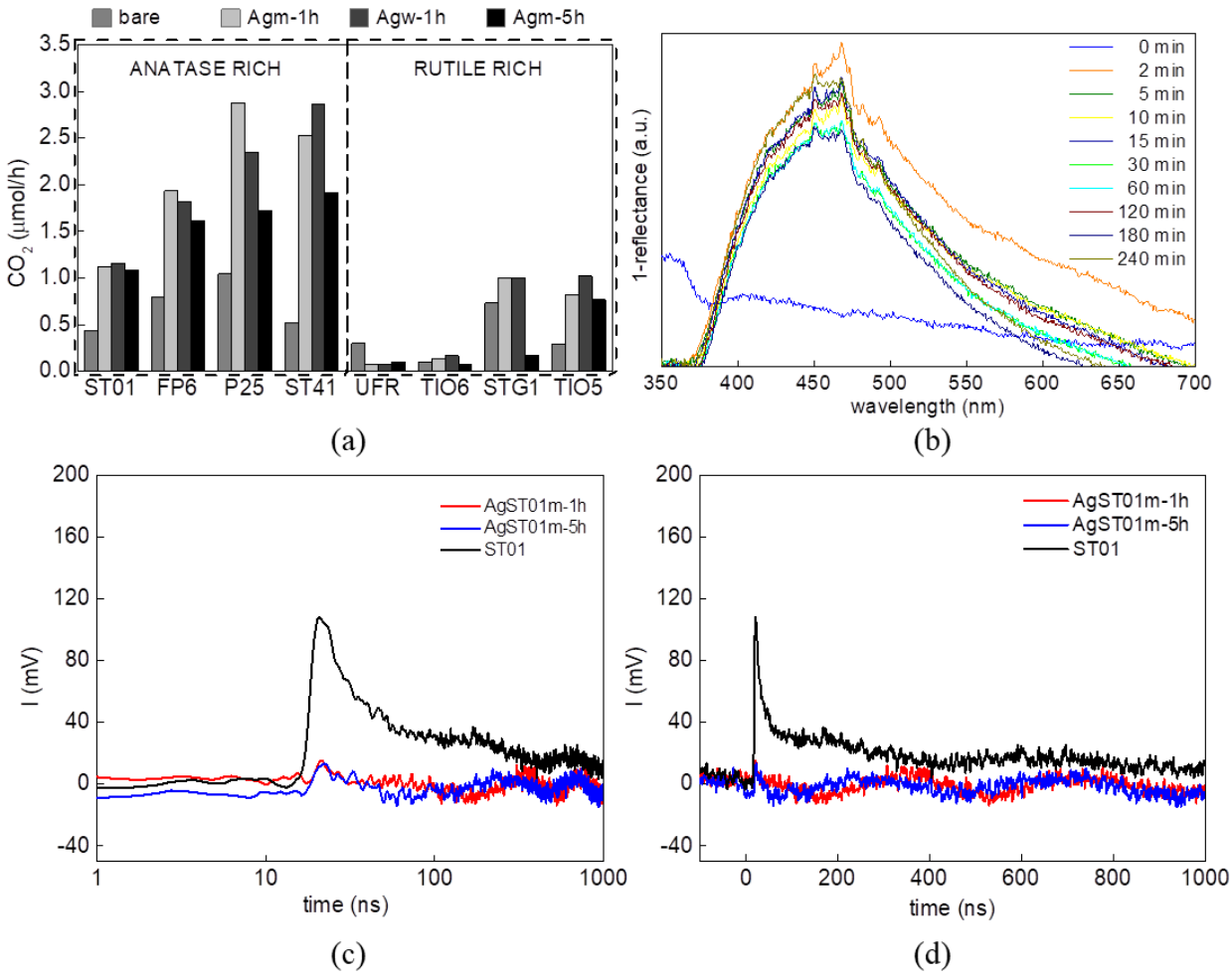

FIG. 7. (**a**) Photocatalytic activity of pristine and silver-modified samples under UV/vis irradiation ($\lambda > 300$ nm), (**b**) DRS of AgST41w-1h suspended in aqueous solution of acetic acid before and after irradiation under UV light, (**c**-**d**) TRMC data for pristine and silver-modified ST01 samples.

Next, the photocatalytic activity under vis irradiation ($\lambda > 450$ nm) was investigated for all samples, and obtained data are presented in Fig. 8a. Obviously, unmodified titania samples are hardly active at this wavelength range. However, their surface modification with silver has caused significant increase (up to 18-fold for AgTIO5m-1h) in the rate of 2-propanol oxidation. In contrast to the activity data taken under UV/vis irradiation, silver-modified large anatase (ST41) exhibits the lowest activity. Generally, higher photocatalytic activity has been observed for the samples prepared in methanol medium, for longer photodeposition duration and containing rutile phase. Similar tendency has been observed for gold-

modified titania samples, where the highest activity under vis irradiation has been obtained for rutile samples with large particle sizes.[22, 27] In those samples, gold NPs of higher polydispersity (size and shape: spherical and rod-like deposits) result in broad plasmon peak (efficient light harvesting), and thus improved photocatalytic activity. Similarly, here, it is thought that longer photodeposition (5 h) resulting in silver aggregation (though not recommended for UV activity, Fig. 7a) might be a key factor of better vis performance (unfortunately no clear plasmonic peak could be observed due to silver oxidation). There are two possibilities of vis-response in the case of silver-modified titania (similar to copper-modified titania case),[28, 38] i.e., plasmonic photocatalysis and heterojunction TiO_2/Ag_xO (x=1-2). The comparison with quite different data obtained for Ag_2O/TiO_2 composites, for which the activity decreases in the following order: large rutile > large anatase (ST41) > fine rutile (TIO6) > mixed phase (P25) > ST01,[28] suggests that the former mechanism (plasmonic photocatalysis) is more probable. Moreover, the aggregation of silver (during longer photodeposition) should be significant disadvantage for heterojunction mechanism (electron transfer from conduction band (CB) of silver oxide to CB of titania) as the interface between titania and silver oxide is crucial for an efficient charge transfer.

Similar to the activity tests under UV irradiation, it has been observed that the color of irradiated suspension has return to brownish (same to that during silver photodeposition), as clearly confirmed by DRS data (Fig. 8b), suggesting that the plasmonic feature might play a crucial role in the mechanism. One of the most active samples (AgTIO5m-1h) was further examined for longer irradiation (and reflectance spectroscopy), as shown in Fig. 8c. Although a good photostability has been observed during 4-h irradiation (with a linear trend), the longer irradiation results in a significant activity loss (ca. 3 times) with simultaneous shift of photoabsorption towards shorter wavelengths (Fig. 8b). Both considered mechanisms might be responsible for the activity loss during longer irradiation, resulting from silver oxidation (electron transfer to CB of titania). Interestingly, though a loss of activity has been observed, the reaction rate after initial 4 h of irradiation is constant (linear trend), indicating the high stability of the photocatalyst under vis irradiation (in contrast to gold-modified titania with no linear vis activity for long-term irradiation).[62] It should be mentioned that in the case of plasmonic photocatalysis, two main mechanisms have been proposed, i.e., charge transfer (hot electrons) and energy transfer.[19, 33, 63, 64] Although in the case of gold-modified titania, the former is more probable considering high differences in activation energy of components (LSPR of ca. 2.3 eV and bandgap of ca. 3.2), in the case of silver-modified titania, the energy transfer from plasmonic silver to titania is highly possible as the overlapping of plasmonic peak and titania photoabsorption is clear (e.g., Fig. 3). Therefore, the high stability (after initial activity decrease – maybe caused by re-shaping of silver deposits, Fig. 8b) of silver-modified titania under vis irradiation suggests the mechanism of plasmonic photocatalysis via energy transfer.

To investigate the mechanism in more detail, TRMC analysis under vis excitation and action spectrum analysis have been investigated. TRMC experiments performed under vis irradiation (430, 470 and 550 nm) does not result in any TRMC peak, as shown in Fig. 8d. Interestingly, the contrary data have been reported for vis responsive photocatalysts, i.e., with or without TRMC signal under vis irradiation.[55, 65-68] The clear TRMC signals under vis excitation have been found in the case of proposed mechanism via electron transfer (either plasmonic or heterojunction), whereas no TRMC signal has been observed for silver-modified titania P25.[68] Therefore, it is thought that the mechanism of energy transfer could be responsible for this observation, i.e., titania is excited via plasmonic energy transfer from silver, and subsequently photo-generated electrons are fast scavenged by silver (similar to the mechanism under UV, causing the lack of TRMC signal, as shown in Fig. 7c-d), and at the same time photo-generated holes oxidize 2-propanol.

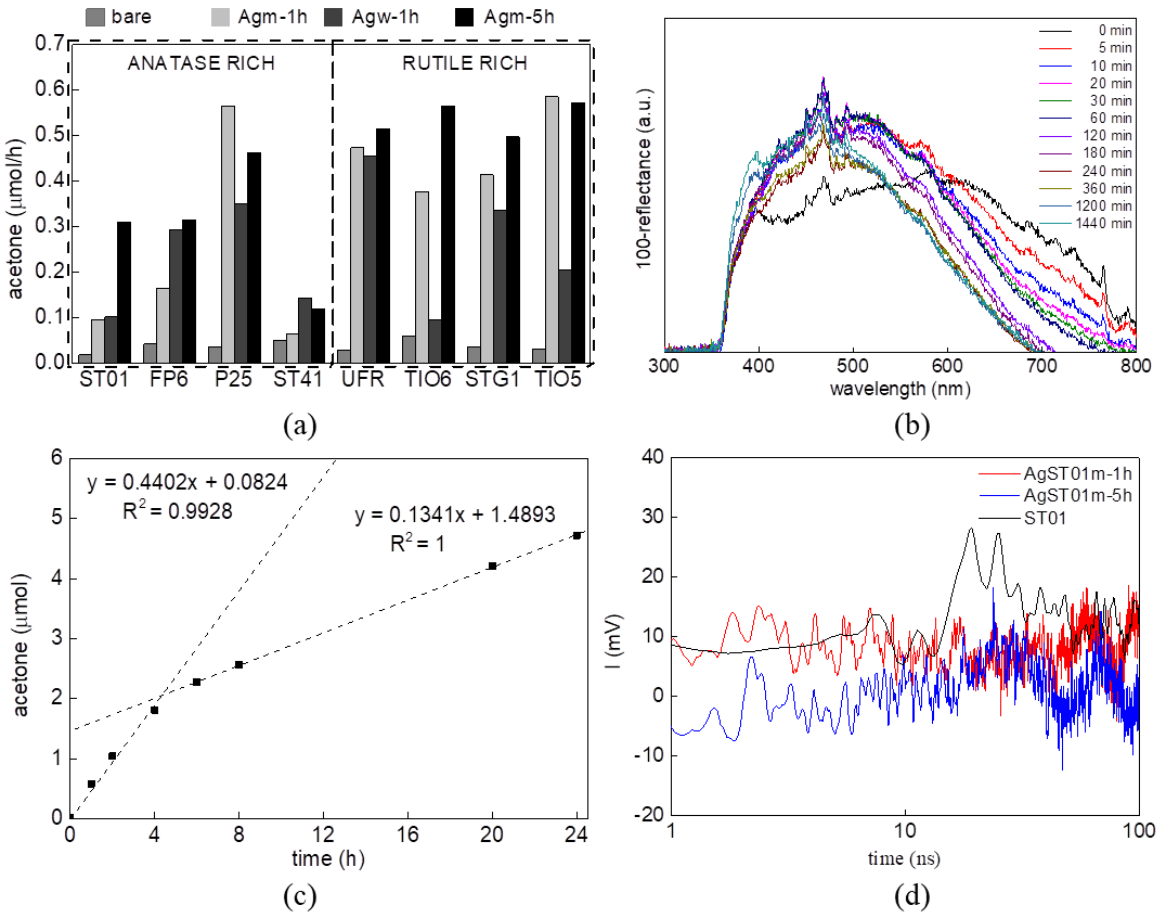

FIG. 8. (**a**) Photocatalytic activity of pristine and silver-modified samples under vis irradiation ($\lambda > 450$ nm), (**b**) diffuse reflectance spectra of AgTIO5m-1h suspended in aqueous solution of 2-propanol before and after irradiation under UV light, (**c**) the stability data for AgTIO5m-1h suspended in aqueous solution of 2-propanol during long-term vis irradiation, (**d**) TRMC data for pristine and silver-modified ST01 samples under excitation at 430 nm.

The action spectra (Fig. 9) are shown together with respective photoabsorption data (taken for irradiated suspension). Unlike DRS taken for dry samples (Fig. 3), photoabsorption under visible light is very limited., i.e., almost without characteristic features of silver oxides (only a small peak at ca. 500 nm for AgTIO5m-1h). Interestingly, action spectra correlate well with photoabsorption spectra, and thus it might be concluded that UV and vis activities are caused by titania excitation and plasmonic photocatalysis, respectively. The negligible activity at longer wavelengths than LSPR of silver confirms that plasmonic photocatalysis rather than TiO_2/Ag_xO heterojunction is responsible for vis response.

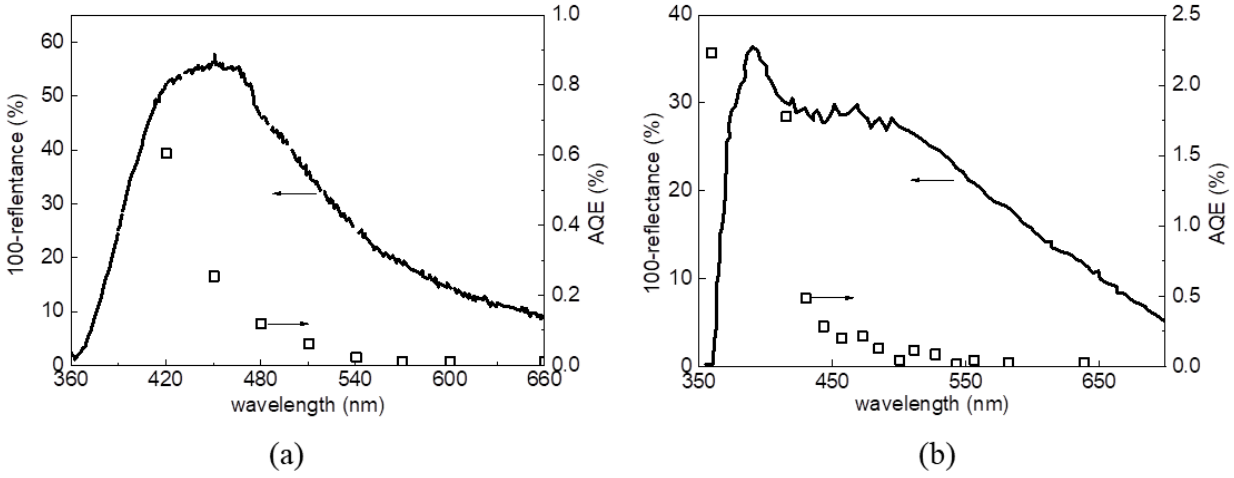

FIG. 9. Action spectra (points) with respective absorption spectra (lines; taken for the suspension) for: (**a**) AgFP6w-1h and (**b**) AgTIO5m-1h samples; AQE – apparent quantum efficiency.

Additionally, the reference experiments were performed, i.e., (i) the activity of silver-modified titania samples for 2-propanol oxidation in the dark and (ii) irradiation of 2-propanol solution in the absence of photocatalyst under vis. It has been confirmed that silver-modified titania is inactive for 2-propanol oxidation in the absence of irradiation, and 2-propanol cannot be oxidized by vis irradiation under the conditions used in this study.

IV. CONCLUSIONS

Modification of titania with silver results in improved activity under both UV and vis irradiation since silver works as an electron scavenger (confirmed by TRMC data) and vis activator, probably by an energy transfer mechanism (as suggested by stability, action spectra and TRMC data).

The obtained activity differs between titania samples significantly, suggesting that the type of crystalline phase, particle/crystallite sizes, and electron traps' density are crucial for both the properties of formed silver deposits and resultant photocatalytic activity.

It should be pointed out that the studies on both silver- and copper-modified titania samples are highly challenging in comparison to gold- and platinum- ones since the co-presence of mixed-oxidation states of these metals (also difficult for precise estimation because of techniques limitations: only crystallites with sufficient content and size by XRD; and only the surface layer by XPS) might result in much complex mechanisms under both UV and vis irradiation, including heterojunction, Z-scheme, plasmonic photocatalysis (energy and/or electron transfer), and the combination of several mechanisms together. Accordingly, it is hardly possible to point out one significant property of silver-modified titania that might cause high photocatalytic performance. Nevertheless, based on presented data, one might conclude that: (i) under UV irradiation high crystallinity and large specific surface area are recommended for rutile- and anatase-rich samples, respectively, during methanol dehydrogenation in the presence of silver in-situ deposition, (ii) mixed crystalline phases result in high rate of oxygen evolution from water during silver UV photodeposition, (iii) anatase phase with fine silver NPs causes efficient oxidative decomposition of acetic acid under UV irradiation, and (iv) aggregated silver NPs (broader LSPR peak) on rutile phase are promising for 2-propanol oxidation under vis irradiation.

Although the correlation between the properties and activities is hardly achieved, it is clear that photocatalytic activities of silver-modified samples are highly dependent on the titania matrix. The conditions of silver deposition influence also the properties of obtained silver deposits, and thus resultant photocatalytic activity, but this impact is not as significant as that by titania matrix. The further studies are necessary to clarify the key factors of photocatalytic activity, and the mechanisms of photocatalytic reactions on silver-modified titania materials.

ACKNOWLEDGEMENTS

Bill & Melinda Gates Foundation through the Grand Challenges Explorations initiative (GCE R8, OPP1060234) and the CONCERT-Japan Joint Call on Efficient Energy Storage and Distribution/Resilience against Disasters are highly acknowledged. The authors thank Professor H. Remita (Université Paris-Saclay, France), Professor S. Rau (Ulm University, Germany) and Professor B. Ohtani (ICAT, Japan) for fruitful discussion and unlimited access to the laboratory facility.

AUTHOR DECLARATIONS

Conflict of Interest

The authors have no conflicts to disclose.

DATA AVAILABILITY

The data that support the findings of this study are available from the corresponding author upon reasonable request.

REFERENCES

1. K. Nakata and A. Fujishima, J Photoch Photobio C **13** (3), 169-189 (2012).
2. K. L. Wang, M. Janczarek, Z. S. Wei, T. Raja-Mogan, M. Endo-Kimura, T. M. Khedr, B. Ohtani and E. Kowalska, Catalysts **9** (12), 1054 (2019).
3. A. Markowska-Szczupak, M. Endo-Kimura, O. Paszkiewicz and E. Kowalska, Nanomaterials-Basel **10** (10), 2065 (2020).
4. B. Tryba, T. Tsumura, M. Janus, A. W. Morawski and M. Inagaki, Appl. Catal. B-Environ. **50** (3), 177-183 (2004).
5. E. Kowalska, H. Remita, C. Colbeau-Justin, J. Hupka and J. Belloni, J. Phys. Chem. C **112** (4), 1124-1131 (2008).
6. H. Kisch, S. Sakthivel, M. Janczarek and D. Mitoraj, J Phys Chem C **111** (30), 11445-11449 (2007).
7. R. Asahi, T. Morikawa, T. Ohwaki, K. Aoki and Y. Taga, Science **293** (5528), 269-271 (2001).
8. T. Ohno, T. Mitsui and M. Matsumura, Chem. Lett. **32** (4), 364-365 (2003).
9. A. Zaleska, Recent Pat. Engin. **2**, 157-164 (2008).
10. K. Wang, Z. Bielan, M. Endo-Kimura, M. Janczarek, D. Zhang, D. Kowalski, A. Zielińska-Jurek, A. Markowska-Szczupak, B. Ohtani and E. Kowalska, J. Mater. Chem. A **9** (16), 10135-10145 (2021).
11. M. Janczarek, M. Endo, D. Zhang, K. Wang and E. Kowalska, Materials. **11**, 2069 (2018).
12. Z. Wang, T. Hu, H. He, Y. Fu, X. Zhang, J. Sun, L. Xing, B. Liu, Y. Zhang and X. Xue, ACS Sustain. Chem. Eng. **6** (8), 10162-10172 (2018).
13. Z. S. Wei, M. Endo-Kimura, K. L. Wang, C. Colbeau-Justin and E. Kowalska, Nanomaterials **9** (10) (2019).
14. F. Amano, O. O. Prieto-Mahaney, Y. Terada, T. Yasumoto, T. Shibayama and B. Ohtani, Chem. Mater. **21** (13), 2601-2603 (2009).
15. D. Kowalski, D. Kim and P. Schmuki, Nano Today **8** (3), 235-264 (2013).
16. B. Kraeutler and A. J. Bard, J. Am. Chem. Soc. **100**, 4317-4318 (1978).
17. P. Pichat, J. M. Herrmann, J. Disdier, H. Courbon and M. N. Mozzanega, Nouv. J. Chim. **5** (12), 627-636 (1981).
18. B. Ohtani, H. Osaki, S. Nishimoto and T. Kagiya, J Am Chem Soc **108** (2), 308-310 (1986).
19. Y. Tian and T. Tatsuma, J Am Chem Soc **127** (20), 7632-7637 (2005).
20. S. W. Verbruggen, J. Photoch. Photobio. C **24**, 64-82 (2015).
21. P. A. DeSario, J. J. Pietron, D. E. DeVantier, T. H. Brintlinger, R. M. Stroud and D. R. Rolison, Nanoscale **5** (17), 8073-8083 (2013).

22. E. Kowalska, R. Abe and B. Ohtani, Chem Commun (2), 241-243 (2009).
23. Z. Wei, M. Janczarek, K. Wang, S. Zheng and E. Kowalska, Catalysts **10** (9), 1070 (2020).
24. E. Kowalska, S. Rau and B. Ohtani, Journal of Nanotechnology, 1-11 (2012).
25. S. W. Verbruggen, M. Keulemans, B. Goris, N. Blommaerts, S. Bals, J. A. Martens and S. Lenaerts, Appl Catal B-Environ **188**, 147-153 (2016).
26. A. Furube, L. Du, K. Hara, R. Katoh and M. Tachiya, J Am Chem Soc **129** (48), 14852-14853 (2007).
27. E. Kowalska, O. O. P. Mahaney, R. Abe and B. Ohtani, Phys. Chem. Chem. Phys. **12** (10), 2344-2355 (2010).
28. M. Endo-Kimura, B. Karabiyik, K. Wang, Z. Wei, B. Ohtani, A. Markowska-Szczupak and E. Kowalska, Catalysts **10** (10), 1194 (2020).
29. E. Kowalska, Z. Wei, B. Karabiyik, A. Herissan, M. Janczarek, M. Endo, A. Markowska-Szczupak, H. Remita and B. Ohtani, Catal Today **252**, 136-142 (2015).
30. N. Sakai, Y. Fujiwara, Y. Takahashi and T. Tatsuma, Chem. Phys. Chem. **10**, 766-769 (2009).
31. W. B. Hou, W. H. Hung, P. Pavaskar, A. Goeppert, M. Aykol and S. B. Cronin, Acs Catal **1** (8), 929-936 (2011).
32. A. M. Pennington, C. L. Pitman, P. A. DeSario, T. H. Brintlinger, S. Jeon, R. B. Balow, J. J. Pietron, R. M. Stroud and D. R. Rolison, Acs Catal **10** (24), 14834-14846 (2020).
33. D. B. Ingram and S. Linic, J Am Chem Soc **133**, 5202-5205 (2011).
34. D. B. Ingram, P. Christopher, J. L. Bauer and S. Linic, Acs Catal **1** (10), 1441-1447 (2011).
35. Y. Horiguchi, T. Kanda, K. Torigoe, H. Sakai and M. Abe, Langmuir **30** (3), 922-928 (2014).
36. Z. Wei, M. Janczarek, M. Endo, K. L. Wang, A. Balcytis, A. Nitta, M. G. Mendez-Medrano, C. Colbeau-Justin, S. Juodkazis, B. Ohtani and E. Kowalska, Appl Catal B-Environ **237**, 574-587 (2018).
37. Z. Wei, M. Endo, K. Wang, E. Charbit, A. Markowska-Szczupak, B. Ohtani and E. Kowalska, Chem. Eng. J. **318**, 121-134 (2017).
38. M. Janczarek, Z. Wei, M. Endo, B. Ohtani and E. Kowalska, Journal of Photonics for Energy **7** (1), 1-16 (2017).
39. M. Janczarek and E. Kowalska, Catalysts **7** (11), 317 (2017).
40. O. O. Prieto-Mahaney, N. Murakami, R. Abe and B. Ohtani, Chem. Lett. **38** (3), 238-239 (2009).
41. A. Nitta, M. Takashima, M. Takase and B. Ohtani, Catal Today **321**, 2-8 (2019).
42. Y.-F. Li, Z.-P. Liu, L. Liu and W. Gao, J Am Chem Soc **132** (37), 13008-13015 (2010).
43. B. Ohtani, O. O. Prieto-Mahaney, D. Li and R. Abe, J Photoch Photobio A **216** (2-3), 179-182 (2010).
44. S. Takeuchi, M. Takashima, M. Takase and B. Ohtani, Chem. Lett. **47** (3), 373-376 (2018).
45. M. J. Sampaio, Z. Yu, J. C. Lopes, P. B. Tavares, C. G. Silva, L. Liu and J. L. Faria, Sci Rep-Uk **11** (1), 21306 (2021).
46. R. Abe, K. Sayama and H. Sugihara, The Journal of Physical Chemistry B **109** (33), 16052-16061 (2005).
47. T. Ohno, K. Sarukawa and M. Matsumura, J. Phys. Chem. B **105** (12), 2417-2420 (2001).
48. Y. Kakuma, A. Y. Nosaka and Y. Nosaka, Phys Chem Chem Phys **17** (28), 18691-18698 (2015).
49. K. L. Wang, Z. S. Wei, B. Ohtani and E. Kowalska, Catal Today **303**, 327-333 (2018).
50. D. Paramelle, A. Sadovoy, S. Gorelik, P. Free, J. Hobley and D. G. Fernig, Analyst **139** (19), 4855-4861 (2014).
51. S. Mukherji, S. Bharti, G. Shukla and S. Mukherji, Physical Sciences Reviews **4** (1) (2019).
52. B. K. Min, W. T. Wallace and D. W. Goodman, Surf. Sci. **600**, L7 (2006).
53. N. Murakami, O. O. P. Mahaney, R. Abe, T. Torimoto and B. Ohtani, J Phys Chem C **111** (32), 11927-11935 (2007).
54. A. Nitta, M. Takase, M. Takashima, N. Murakamid and B. Ohtani, Chem Commun **52** (81), 12096-12099 (2016).

55. M. G. Mendez-Medrano, E. Kowalska, A. Lehoux, A. Herissan, B. Ohtani, D. Bahena, V. Briois, C. Colbeau-Justin, J. Rodriguez-Lopez and H. Remita, The Journal of Physical Chemistry C **120**, 5143-5154 (2016).
56. M. Endo-Kimura, M. Janczarek, Z. Bielan, D. Zhang, K. Wang, A. Markowska-Szczupak and E. Kowalska, ChemEngineering **3** (1), 3 (2019).
57. C. Colbeau-Justin, M. Kunst and D. Huguenin, J Mater Sci **38** (11), 2429 (2003).
58. K. Wang, K. Yoshiiri, L. Rosa, Z. Wei, S. Juodkazis, B. Ohtani and E. Kowalska, Catal Today, in press (2022) doi: 10.1016/j.cattod.2021.09.023.
59. B. Ohtani, O. O. P. Mahaney, F. Amano, N. Murakami and R. Abe, J Adv Oxid Technol **13** (3), 247-261 (2010).
60. N. Murakami, O. O. P. Mahaney, T. Torimoto and B. Ohtani, Chem. Phys. Lett. **426** (1-3), 204-208 (2006).
61. M. Buchalska, M. Kobielusz, A. Matuszek, A. Pacia, S. Wojtyla and W. Macyk, ACS Catal. **5** (12), 7424–7431 (2015).
62. K. Wang, K. Yoshiiri, L. Rosa, Z. Wei, S. Juodkazis, B. Ohtani and E. Kowalska, Catal Today (2021).
63. L. C. Du, A. Furube, K. Yamamoto, K. Hara, R. Katoh and M. Tachiya, J Phys Chem C **113** (16), 6454-6462 (2009).
64. W. B. Hou and S. B. Cronin, Adv Funct Mater **23** (13), 1612-1619 (2013).
65. M. G. Mendez-Medrano, E. Kowalska, B. Ohtani, D. B. Uribe, C. Colbeau-Justin, S. Rau, J. L. Rodriguez-Lopez and H. Remita, J Chem Phys **153** (3), 034705 (2020).
66. A. L. Luna, D. Dragoe, K. L. Wang, P. Beaunier, E. Kowalska, B. Ohtani, D. B. Uribe, M. A. Valenzuela, H. Remita and C. Colbeau-Justin, J Phys Chem C **121** (26), 14302-14311 (2017).
67. E. Kowalska, K. Yoshiiri, Z. Wei, S. Zheng, E. Kastl, H. Remita, B. Ohtani and S. Rau, Appl. Catal. B: Environ. **178**, 133-143 (2015).
68. E. Grabowska, A. Zaleska, S. Sorgues, M. Kunst, A. Etcheberry, C. Colbeau-Justin and H. Remita, J Phys Chem C **117** (4), 1955-1962 (2013).